Heliyon 5 (2019) e02367

Contents lists available at ScienceDirect

Heliyon

journal homepage: www.heliyon.com

VDR agonists down regulate PI3K/Akt/mTOR axis and trigger autophagy in Kaposi's sarcoma cells

Alejandra Suares [a,b], Cinthya Tapia [a], Verónica González-Pardo [a,*]

[a] Instituto de Ciencias Biológicas y Biomédicas del Sur (INBIOSUR), Departamento de Biología Bioquímica y Farmacia, Universidad Nacional del Sur (UNS)-CONICET, San Juan 670, 8000, Bahía Blanca, Argentina

[b] IFIBYNE – Instituto de Fisiología, Biología Molecular y Neurociencias (UBA-CONICET), Ciudad Universitaria, 1428, Ciudad Autónoma de Buenos Aires, Argentina

ARTICLE INFO

Keywords:
Biochemistry
Molecular biology
Cancer research
Endocrinology
Active vitamin D
Akt
Beclin-1
Autophagy
vGPCR
Endothelial cells

ABSTRACT

The Kaposi's sarcoma-associated herpesvirus G protein-coupled receptor (KSHV/vGPCR) is a key molecule in the pathogenesis of Kaposi's sarcoma. We have previously shown that 1α,25(OH)$_2$D$_3$ or its less-calcemic analog TX 527 inhibits the proliferation of endothelial cells expressing vGPCR, NF-κB activity and induces apoptosis in a VDR dependent manner. In this work, we further explored whether 1α,25(OH)$_2$D$_3$ or TX 527 regulates PI3K/Akt/mTOR axis and induces autophagy as part of its antineoplastic mechanism of action. Proliferation assays indicated that vGPCR cell number decreased in presence of LY294002 (PI3K/Akt inhibitor) likewise 1α,25(OH)$_2$D$_3$ or TX 527 (10 nM, 48 h). Also, Akt phosphorylation was found decreased in dose (0.1–100 nM) and time response studies (12–72 h) after both compounds treatments. In addition, decreased phosphorylated Akt was significantly observed in the nucleus. Moreover, regulation of Akt phosphorylation was NF-κB and VDR dependent. TNFAIP3/A20, an ubiquitin-editing enzyme, a direct NF-κB target gene and a negative regulator of Beclin-1, was down-regulated whereas Beclin-1 was up-regulated after 10 nM of 1α,25(OH)$_2$D$_3$ or TX 527 treatment. Decrement in Akt phosphorylation was accompanied by a reduced mTOR phosphorylation and an increase in the autophagy marker LC3-II. Since increment in autophagosomes not always indicates increment in autophagy activity, we used Chloroquine (CQ, 1 μM), an inhibitor of autophagy flow, to confirm autophagy after both VDR agonists treatment. In conclusion, VDR agonists, 1α,25(OH)$_2$D$_3$ or TX 527, inhibited PI3K/Akt/mTOR axis and induced autophagy in endothelial cells expressing vGPCR by a VDR-dependent mechanism.

1. Introduction

Kaposi sarcoma-associated herpesvirus (KSHV, HHV-8) is a tumorigenic γ-herpesvirus [1] and provokes the development of three human malignancies. In endothelial cells, promotes Kaposi's sarcoma (KS) and in B-cells, two lympho-proliferative diseases: primary effusion lymphoma and the plasma cell variant of multicentric Castleman's disease [2]. These diseases appear primarily in the context of immune deficiency and/or HIV infection, though their pathogenesis differs [2]. KS is a multifocal, highly vascular tumor; cells display features of activated endothelial cells, and develops on the lower extremities, mucous membranes or internal organs [1, 3]. KSHV encodes several oncogenic viral homologues of host proteins with the potential to stimulate cell survival, proliferation, immune evasion and angiogenesis [4, 5, 6]. Among them, the viral G protein-coupled receptor (vGPCR) has shown to transform endothelial cells due to its pro-angiogenic capacity promoting tumor growth [3, 4, 5, 7]. The vGPCR is encoded by the ORF74, and presents homology with CXCR1 and CXCR2, receptors of IL-8 and Gro-α in the host [3, 8, 9]. This viral receptor is constitutively active because of the presence of structural changes within its DRY domain in the second intra-cytoplasmic loop, which is highly conserved in GPCRs [4, 10]. Among the multiple intracellular pathways stimulated by vGPCR, the Akt/mTOR signaling axis represents one of the most prominent oncogenic mechanism activated, an event that has been revealed by animal models of KS [7, 11]. vGPCR activates Akt/mTOR by stimulating PI3K through βγ-subunits and by an autocrine manner up-regulating VEGFR2/KDR expression and VEGF release [4, 12]. Moreover, PI3Kγ has been identified as the activator of Akt/mTOR in endoth elial cells expressing vGPCR and also to mediate sarcomagenesis *in vivo* [13].

It is well documented the important role of the PI3K/Akt pathway in cell growth, proliferation, survival and metabolism [14]. In cancer cells, it plays a central role in aerobic glycolytic reprogramming, tumor

* Corresponding author.
E-mail address: vgpardo@criba.edu.ar (V. González-Pardo).

https://doi.org/10.1016/j.heliyon.2019.e02367
Received 7 March 2019; Received in revised form 14 May 2019; Accepted 21 August 2019

growth, and survival [15]. mTOR, a major intracellular repressor of autophagy, is positively regulated by the PI3K/Akt pathway [16].

Autophagy is a mechanism that mediates the sequestration of cytoplasmic material in autophagosomes, double membrane vesicles, that in turn fuse to lysosomes for degradation [17, 18]. Autophagy not only occurs under normal conditions to maintain cell homeostasis, but also during unfavorable conditions [16, 19]. In neoplastic cells, autophagy constitutes a mean to face intracellular and environmental stress, thus favoring tumor progression [18]. There are several autophagy inducers that operate in general activating cascades of signal transduction that result in mTOR complex 1 inhibition [20, 21]. Among other effects, this allows the activation of proteins that are crucial in autophagosomes formation, such as ULK-1, ATG13 and Beclin-1 (BECN1) [18,22]. Autophagy is governed by a series of Atg genes [16, 18, 23]. Although all ATG8 proteins are indispensable for autophagy, LC3 acts as the major ATG8 protein to induce autophagy; thus, increased levels of LC3-II proteins in autophagosome membranes are important biomarkers of autophagy [16, 24].

The active form of vitamin D, 1α, 25 $(OH)_2$-vitamin D_3 ($1\alpha,25(OH)_2D_3$) or calcitriol plays an important role in maintaining calcium homeostasis. Most of $1\alpha,25(OH)_2D_3$ actions are mediated through the vitamin D receptor (VDR), a member of the nuclear receptor superfamily [25]. In addition to its classical effects, $1\alpha,25(OH)_2D_3$ has antineoplastic and anti-inflammatory effects in several tumor types. The anti-proliferative, pro-apoptotic and pro-differentiation action of the metabolite has been demonstrated in various malignant cells and also in animal models where it retards tumor growth [26, 27, 28, 29, 30, 31]. We have previously revealed that $1\alpha,25(OH)_2D_3$ or its less-calcemic analog TX 527 inhibits the proliferation of endothelial cells expressing vGPCR *in vitro* and *in vivo* [32], down regulates NF-κB pathway, highly activated by the viral receptor [33, 34], and induces apoptosis in a VDR dependent manner [35, 36]. Since there is evidence indicating that $1\alpha,25(OH)_2D_3$ triggers autophagy as part of its mechanism of action in certain tumor cells [37, 38, 39], we further explore whether $1\alpha,25(OH)_2D_3$ or TX 527 induces autophagy in endothelial cells expressing vGPCR by inhibiting PI3K/Akt/mTOR pathway.

2. Materials and methods

2.1. Materials

Vitamin D analog TX 527 [19-nor-14,20-bisepi-23-yne-$1,25(OH)_2D_3$] was originally synthesized by M. Vandewalle and P. De Clercq (University of Ghent, Ghent, Belgium) and provided by Théramex (Monaco). Immobilon P (polyvinylidenedifluoride; PVDF) membranes, $1\alpha,25(OH)_2D_3$, the antibiotic G418 and LY294002 were from Sigma-Aldrich (St. Louis, MO, USA). Puromycin supplied by Invivogen (San Diego, CA, USA). The antibodies used were rabbit monoclonal anti-p-Akt, anti-Akt, anti-MEKα (Cell Signaling Technology, Danvers, MA, USA) and anti-Tubulin (Thermo Fisher Scientific Inc., Waltham, MA, USA); mouse monoclonal anti-LC3, anti-BECN1, anti-p-mTOR, and anti-mTOR, goat polyclonal Lamin B and secondary antibodies anti-rabbit, anti-mouse and anti-goat (Santa Cruz Biotechnology, Santa Cruz, CA, USA). Roche Applied Science supplied high Pure RNA Isolation Kit (Indianapolis, IN, USA). High Capacity cDNA RT and SYBR Green PCR Master Mix reagent (Applied Biosystems) were acquired from Thermofisher (Thermofisher, Buenos Aires, AR). GAPDH primer was from Invitrogen™ (Invitrogen/Thermo Fisher Scientific Inc., Waltham, MA, USA) and BECN1 primer was obtained by Eurogentec (Serain, Belgium). The inhibitor of flux autophagy, Chloroquine, was kindly provided by Dr. Daniel Grasso (IBIMOL Universidad de Buenos Aires – CONICET).

2.2. Cell lines and transfections

SV-40 immortalized murine endothelial cells (SVEC) stably expressing the vGPCR (full-length) were used as experimental model of KS [3, 32]. Cells were cultured and selected with 500 μg mL^{-1} G418 [3]. Stable vGPCR endothelial cells targeted with small hairpin RNA against mouse VDR (vGPCR-shVDR) or control shRNA (vGPCR-shctrl) were obtained before by transduction of lentiviral particles generated in HEK293T cells and selected with 2 μg mL^{-1} puromycin [32].

2.3. Proliferation assays

vGPCR cells were seeded in 24-well plates, at 6000 cells per well. After overnight growth, the cells were starved for 24 h and then treated with 10 nM of $1\alpha,25(OH)_2D_3$ or TX 527 or vehicle (0.01%, ethanol) in triplicate in DMEM 2% fetal bovine serum (FBS) for 48 h. Cells were then harvested and counted in a Neubauer chamber using 0,4% of trypan blue stain to distinguish living from died cells according to trypan blue exclusion test [40] In addition, proliferation was measured using CellTiter 96® AQueous one solution cell proliferation assay containing 3-(4, 5-dimethylthiazol-2-yl)-5-(3-carboxymethoxyphenyl)-2- (4-sulfophenyl)-2H-tetrazolium, inner salt (MTS) in 96-well plates as we have previously reported [34].

2.4. SDS-PAGE and Western blot

Whole protein lysates were prepared as previously reported by us [33] and protein content was determined by the Bradford procedure [41]. Proteins were resolved (with SDS–PAGE) and transferred to PVDF membranes followed by Western blot analyzes [41]. Membranes were blocked and incubated with primary antibodies [anti: p-Akt (1:1000), Akt (1:1000), Tubulin (1:1000), MEKα (1:1000), Lamin B (1:1000), BECN1 (1:500), LC3 (1:500), p-mTOR (1:500), mTOR (1:500)] diluted in TBST buffer (0.1% tween) overnight at 4 °C. After three washes in TBST buffer, membranes were incubated with the corresponding secondary antibodies (1:5000) diluted in TBST buffer (2.5% dry milk) 1 h at room temperature. Later, after three washes in TBST buffer, blot signal was detected using an enhanced chemiluminescence kit according to the manufacturer's instructions (Amersham ECL Western Blotting Detection Kit, GE Healthcare, Buenos Aires, AR). Images were scanned and quantified using ImageJ software, developed at the National Institutes of Health.

2.5. Subcellular fractionation

vGPCR cells were scrapped in ice-cold Tris-EDTA-Sucrose (TES) buffer (50 mmol L^{-1}Tris-HCl pH 7.4, 1 mmol L^{-1} EDTA, 250 mmol L^{-1} sucrose, 1 mmol L^{-1} DTT) containing proteases inhibitors (0.5 mmol L^{-1} PMSF, 20 μg mL^{-1} aprotinin and 20 μg mL^{-1} leupeptin). Lysates were passed through a 25 G needle 10 times using a 1 mL syringe and left on ice for 20 min. Then, homogenate was centrifuged at 100 g for 5 min to eliminate debris; supernatant was further centrifuged at 1500 g for 20 min to sediment the nuclear fraction. The supernatant was further centrifuged at 14000 g for 20 min to pellet mitochondria. The remaining supernatant was collected as cytosol fraction [42]. Protein concentration from each fraction was estimated by the Bradford method. Goat anti-Lamin B and rabbit anti-MEKα antibodies were employed for the immunodetection of the nuclear protein marker Lamin B and the cytosol protein marker MEKα, in the different fractions.

2.6. Quantitative real-time PCR

Total RNA for real-time quantitative reverse transcriptase polymerase chain reaction (qRT-PCR) analysis was isolated using the High Pure RNA Isolation Kit (Roche) [34]. Total RNA (1 μg) was reverse transcribed using the kit High Capacity cDNA RT (Applied Biosystems, Thermofisher, Buenos Aires, AR) and qRT-PCR reactions were achieved on the resulting cDNA (5–10 ng) in an ABI 7500 Real Time PCR system (Applied Biosystems, CA, USA) using specific primers to detect A20 and BECN1 levels and GAPDH to normalize gene expression. Primers used for amplification were: murine *Gapdh,* forward 5′-AAGGTGAAGGTCGGAGTC-3′, reverse

5′-GAAGATGGTGATGGGATTTC-3′; murine *Becn1,* forward 5′-GGACAAGCTCAAGAAAACCAATG-3′, reverse 5′-TGTCCGCTGTGCCA-GATG-3'; murine *A20* forward 5′-CATGAAGCAAGAAGAACGGAAGA-3′, reverse 5′-GAGGCCCGGGCACATT-3'. Reactions were carried out using the SYBR Green PCR Master Mix reagent (Applied Biosystems). Gene expression was then analyzed by 2-delta delta Ct method [43].

2.7. Statistical analysis

Data are shown as means ±aSD. Data from control and treated conditions obtained by qRT-PCR or Western blot were analyzed by the two tailed t-test. A p value <0.01 (**) and <0.05 (*) were considered statistically significant. Data from more than two conditions were analyzed by one-way ANOVA followed by Bonferroni test. Different superscript letters indicate significant differences at $p < 0.05$ or $p < 0.01$.

3. Results

3.1. Akt inactivation reduces vGPCR cell number likewise 1α,25(OH)$_2$D$_3$ or TX 527

In a cellular model of KS, Martin and colleagues reported that vGPCR expression in endothelial cells strongly stimulates Akt (pAkt S473) and mTOR, event that was accompanied by morphological changes with an increase in cell size and a longer survival of cells after growth factors deprivation [44]. We first investigated whether 1α,25(OH)$_2$D$_3$ or TX 527 exerts its anti-proliferative effect through the regulation of Akt in endothelial cells transformed by vGPCR. To that end, vGPCR cells were treated with 10 nM of 1α,25(OH)$_2$D$_3$ or TX 527 or 10 μM of LY294002 (PI3K/Akt inhibitor) or vehicle (0.01% ethanol) for 48 h. After treatment, micrographs of each condition were taken in a phase contrast microscope (Fig. 1A). To measure cell proliferation, cells were collected, counted in a Neubauer chamber and, finally, living cells percentage was calculated according to control cells (Fig. 1B). As can be seen from Fig. 1, vGPCR cells number decreased significantly in presence of LY294002 similar to 1α,25(OH)$_2$D$_3$ or TX 527. Furthermore, these results were confirmed by the 3-(4, 5-dimethylthiazol-2-yl)-5-(3-carboxymethoxyphenyl)-2-(4-sulfophenyl)-2H-tetrazolium, inner salt assay (Fig. 1C). In addition, these effects were accompanied by cellular morphological changes, observed by light field microscopy showed abnormal round cells and condensed nuclei, presuming that Akt inhibition is part of both compounds antineoplastic action. To evaluate this possibility, Akt phosphorylation state was studied as a measure of its activity in dose and time response studies. vGPCR cells were treated with increasing concentrations

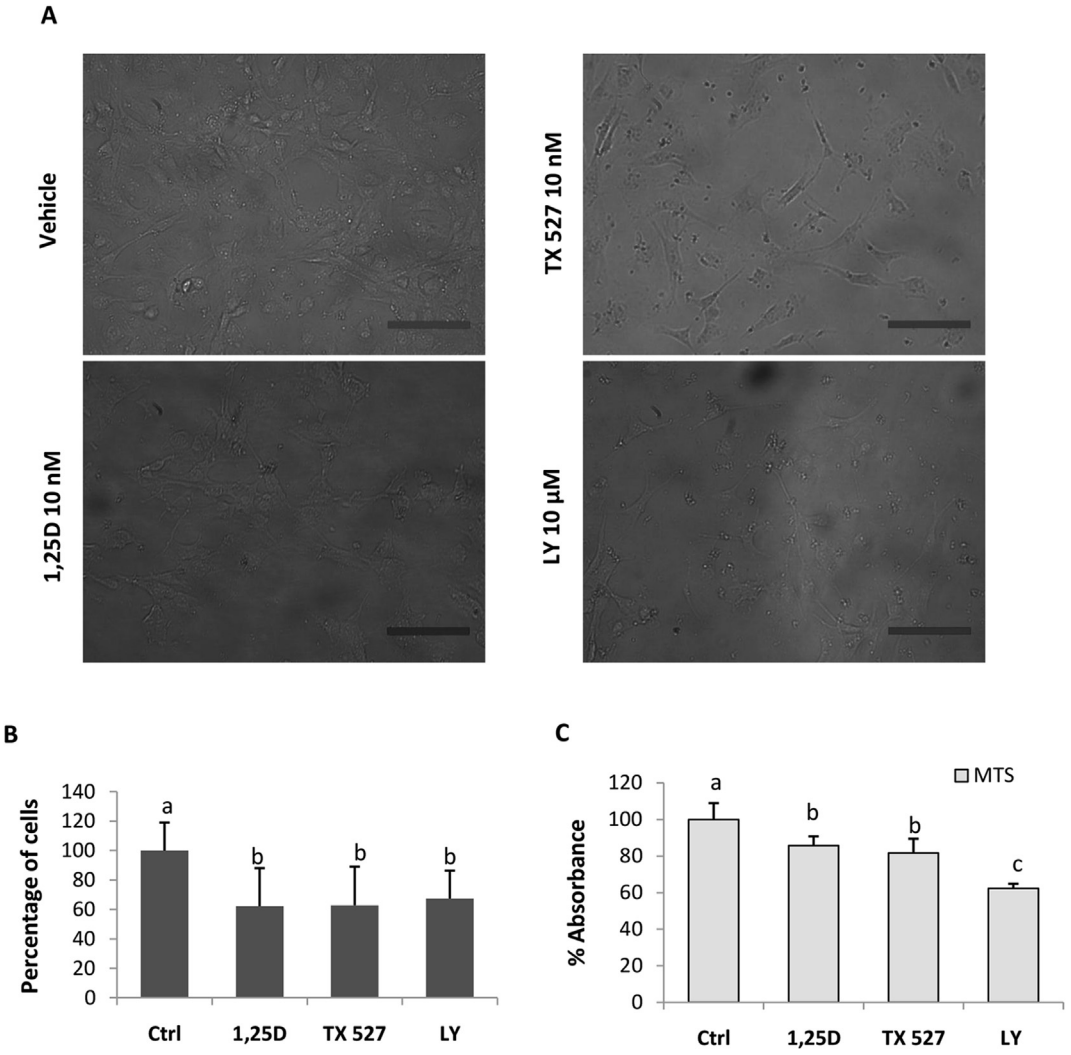

Fig. 1. vGPCR cell growth inhibition by LY294002 and VDR agonists. vGPCR cells were seeded and treated with 10 nM of 1α,25(OH)$_2$D$_3$ (1,25D) or TX 527 or vehicle (0.01% ethanol) or 10 μM of LY294002 (LY) for 48 h. A) Representative micrographs obtained by phase contrast microscopy, bar: 30 μm, magnification 200x. B) Cells were counted in Neubauer chamber or C) in parallel experiments, MTS assay was performed, and the results, from at least three independent experiments, were presented in bar graphs. The statistical analysis was performed by one-way ANOVA followed by the Bonferroni test. Significant differences are indicated by different letters ($p < 0.01$).

of 1α,25(OH)$_2$D$_3$ or TX 527 (0.1–100 nM) or vehicle (0.01% ethanol) for 48 h or with 10 nM of each compound for different times (12–72 h). Then, Akt protein levels and its phosphorylation state were analyzed by Western blot. The results presented in Fig. 2A show that both compounds caused a significant decrease in Akt phosphorylation without modifying its total protein levels in a dose-dependent manner. In addition, time-response studies revealed that Akt phosphorylation significantly decreased after 12–72 h of 1α,25(OH)$_2$D$_3$ or TX 527 treatment (Fig. 2B).

3.2. 1α,25(OH)$_2$D$_3$ inhibits the translocation of phosphorylated Akt to the nucleus

To inquire into 1α,25(OH)$_2$D$_3$ mechanism of action on Akt regulation, we next investigated whether the observed decrease in Akt phosphorylation affects its subcellular location. For this, vGPCR cells were treated with 10 nM of 1α,25(OH)$_2$D$_3$ or vehicle (0.01% ethanol) for 48 h. Then, cells were collected, homogenized in TES buffer and a subcellular

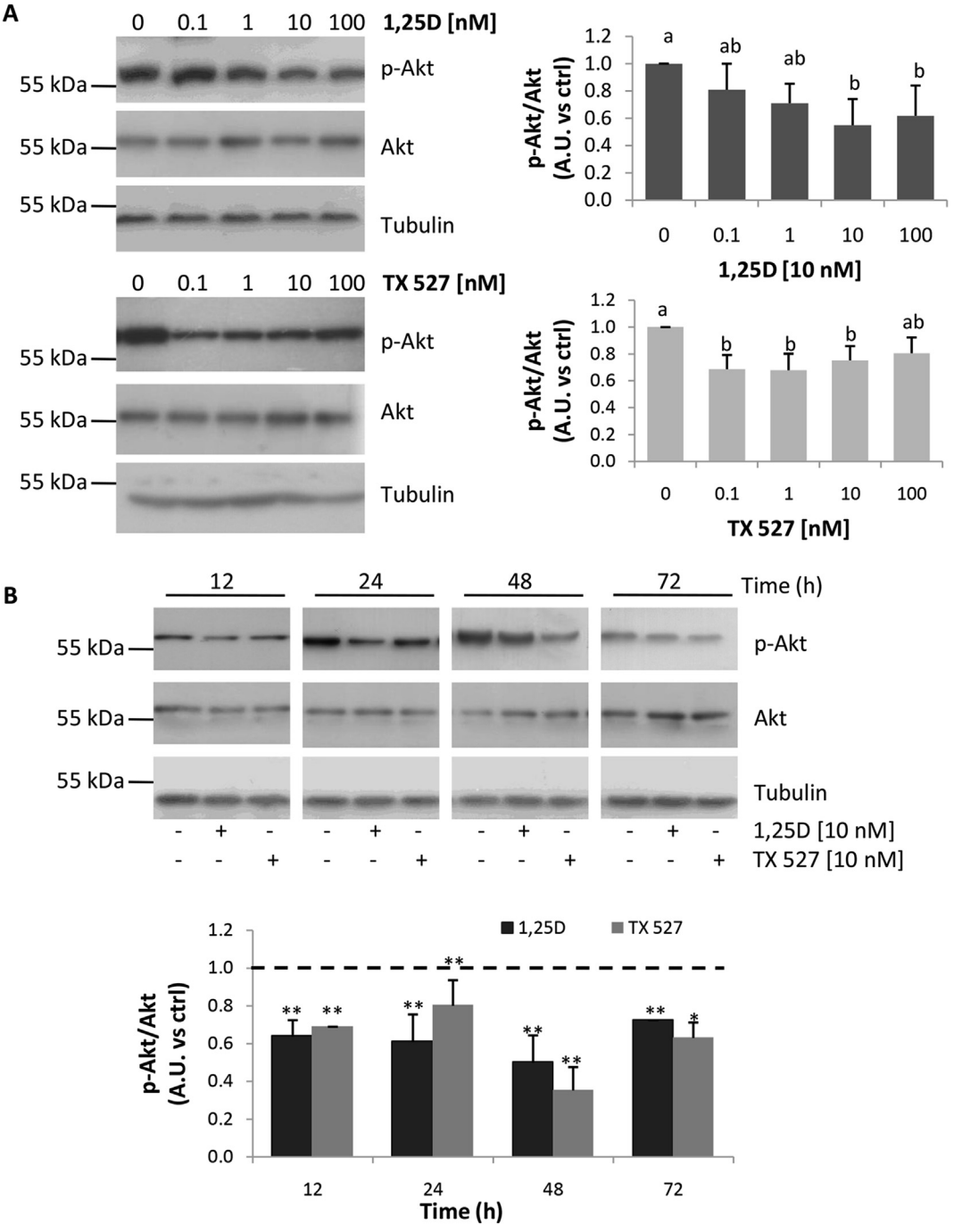

Fig. 2. 1α,25(OH)$_2$D$_3$ or TX 527 decreases Akt phosphorylation in a dose and time dependent manner. vGPCR cells were treated with A) increasing concentrations of 1α,25(OH)$_2$D$_3$ (1,25D) or TX 527 (0–100 nM), or vehicle (0.01% ethanol) for 48 h or B) 10 nM of 1,25D or TX 527 or vehicle (0.01% ethanol) at different times (12–72 h). Total and phosphorylated Akt was analyzed by Western blot and Tubulin was used as loading control. In A and B a representative blots of at least three independent experiments and their quantification in bar graphs are shown. The statistical analysis in A was performed by one-way ANOVA followed by the Bonferroni test. Different letters indicate significant differences between conditions with $p < 0.01$; and in B the effect of each treatment (1,25D or TX 527) was compared with control at each time point by the Student's t test (*$p < 0.05$; **$p < 0.01$). Full, non-adjusted and uncropped images of Fig. 2 are shown in suppl. material.

fractionation was performed to obtain the nuclear and cytosol fraction. Phosphorylated and total Akt levels were analyzed by Western blot and the purity of the fractions was determined through specific markers, Lamin B for nucleus and MEKα for cytosol. The results in Fig. 3 indicate that 1α,25(OH)$_2$D$_3$ provoked a significant decrease in phosphorylated Akt in the nucleus respect to cytosol (Fig. 3B) suggesting the attenuation of Akt activity in the nucleus due to 1α,25(OH)$_2$D$_3$ treatment and its translocation to cytosol (Fig. 3C).

3.3. 1α,25(OH)$_2$D$_3$ or TX 527 decreases Akt activation by a VDR dependent mechanism

Like other steroid hormones, 1α,25(OH)$_2$D$_3$ exerts its effect through a genomic mechanism mediated by VDR and a non-genomic one of rapid responses initiated in the membrane [45]. Therefore, we investigated whether VDR knockdown affects Akt activation. We used the vGPCR-shVDR cell line where VDR expression was silenced by a short hairpin against mouse VDR, or the control line, vGPCR-shctrl. Both cell lines were treated with 10 nM of 1α,25(OH)$_2$D$_3$ or TX 527 or vehicle (0.01% ethanol) for 48 h (Fig. 4A). First, VDR knockdown was verified as we have reported before (Suppl. Material) (Gonzalez Pardo et al., 2010, Gonzalez Pardo et al 2014). Second, as it was previously observed, 1α, 25(OH)$_2$D$_3$ or TX 527 significantly decreased Akt phosphorylation after 48 h of treatment, whereas when VDR expression was knockdown, Akt phosphorylation was not affected by both agonists.

3.4. Inhibition of NF-κB pathway by Bortezomib decreases Akt phosphorylation like VDR agonists

Results from our group have revealed that the inhibition of the NF-κB pathway by Bortezomib plays an important role in the regulation of the cell cycle [34]. This regulation could be attributed to an inhibition of Akt activity by NF-κB. To evaluate this possibility, vGPCR cells were treated with increasing concentrations of Bortezomib (0.25–1 nM) or vehicle (0.1% DMSO) for 24 h and then Akt phosphorylation state was assessed by Western blot. The results presented in Fig. 4B indicate that Bortezomib induced a significant decrease of Akt phosphorylation in a dose-dependent manner; however, at the highest concentration of 1 nM, Akt phosphorylation tended to increase, suggesting that activated Akt contribute to activate cell survival and counteract the apoptosis induced by Bortezomib.

3.5. A20 is highly expressed in vGPCR cells and is down-regulated by 1α,25(OH)$_2$D$_3$ or TX 527

TNFAIP3/A20 is an ubiquitin-editing enzyme and a direct NF-κB

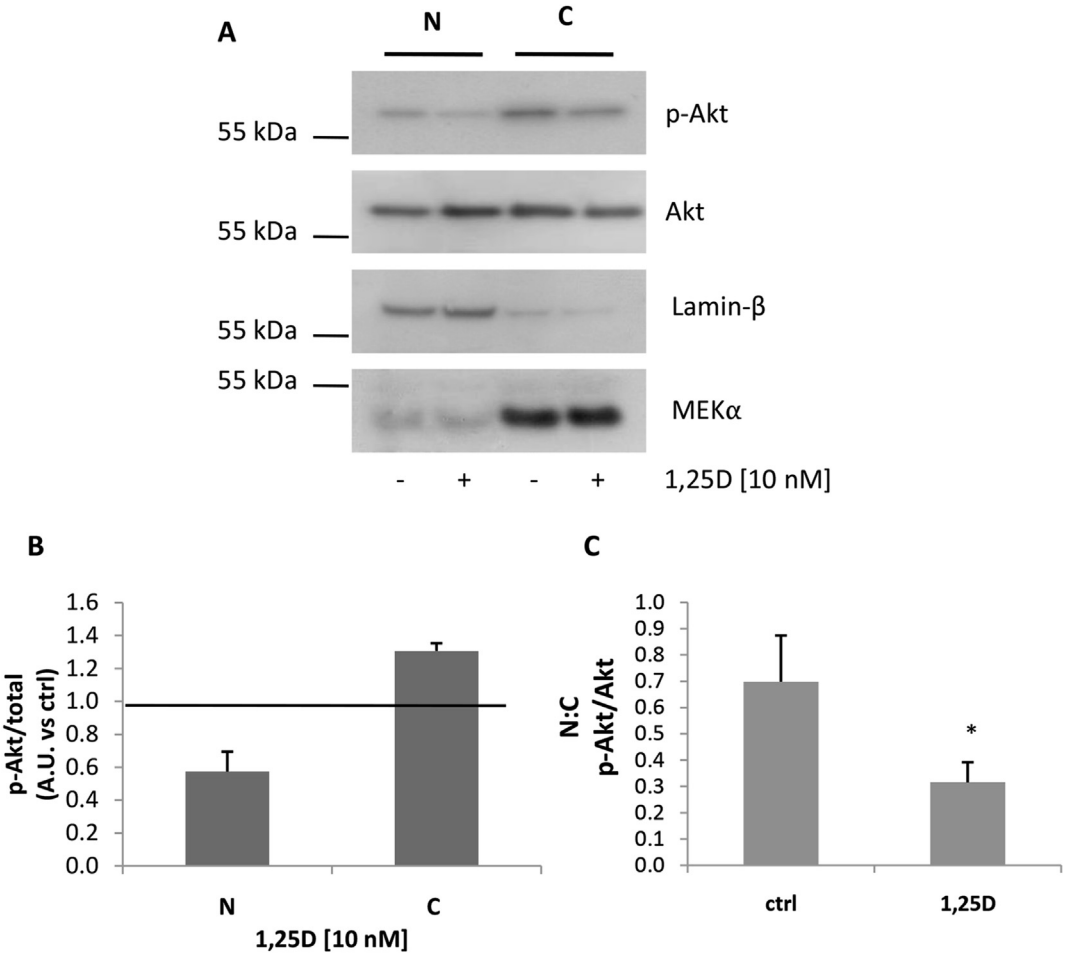

Fig. 3. Subcellular localization of Akt by 1α,25(OH)$_2$D$_3$. vGPCR cells were cultured and treated with 10 nM of 1α,25(OH)$_2$D$_3$ (1,25D) or vehicle (0.01% ethanol) for 48 h. Then, cells were collected in TES buffer and a subcellular fractionation was performed to obtain the nuclear fraction (N) and the cytosol (C). The levels of phosphorylated and total Akt and specific markers for each fraction, MEKα for C and Lamin B for N, were analyzed by Western blot. Representative blots of three independent experiments are shown and their quantification is represented in a bar graph where the radio of p-Akt/Total is expressed in N with respect to C (N: C). Statistical analysis was performed by the Student's t-test, significant differences between the 1,25D and control were evaluated (*$p < 0.05$). Full, non-adjusted and uncropped images of Fig. 3 are shown in suppl. material.

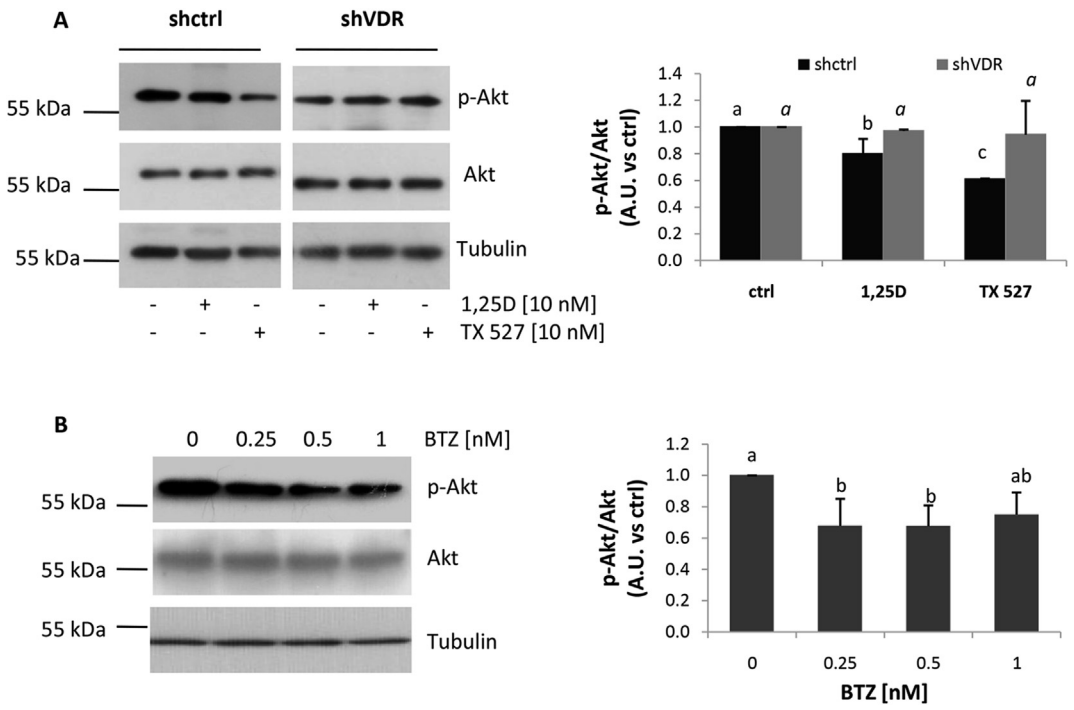

Fig. 4. Decreased Akt phosphorylation is VDR and NF-κB dependent. A) vGPCR-shctrl (shctrl) and vGPCR-shVDR (shVDR) cells were cultured and treated with 10 nM of 1α,25(OH)$_2$D$_3$ (1,25D) or TX 527 or vehicle (0.01% ethanol) for 48 h. B) vGPCR cells were treated with Bortezomib (0.25–1 nM) or vehicle (DMSO, 0.1%) for 24 h. Phosphorylated and total Akt levels were evaluated by Western blot and Tubulin was used as loading control. Representative blots of at least three independent experiments and their quantification plotted on a bar graph are shown. Full, non-adjusted and uncropped images and VDR silencing are shown in suppl. material. The statistical differences were analyzed by one-way ANOVA followed by the Bonferroni test. Different letters indicate significant differences ($p < 0.05$).

target gene that is thought to be a negative regulator of autophagy in some cell lines [46]. It has been proposed that A20 expression limits TLR4-induced autophagy by deubiquitinating TRAF6 and BECN1 [47]. In earlier studies, we have demonstrated that NF-κB is highly expressed in vGPCR cells and is down regulated by VDR agonists [33, 34]. Here, we investigated A20 expression in SVEC and vGPCR cells and whether it was regulated by NF-κB inhibitor Bortezomib or VDR agonists as part of their mechanism of action (Fig. 5). First, SVEC and vGPCR cells were cultured and treated with Bortezomib at different concentrations or vehicle (DMSO, 0.1%) during 24 h and then A20 protein levels were analyzed by Western blot. According to Fig. 5A, A20 was barely expressed in SVEC cells whereas was found highly expressed in vGPCR and down-regulated by Bortezomib in a dose-response manner. Secondly, dose (0.1–100 nM) (Fig. 6) and time response studies (10 nM, 3–72 h) were carried out to investigate the role of 1α,25(OH)$_2$D$_3$ or TX 527 on A20 expression (Fig. 5B and C). The results of these studies indicated that both compounds decreased A20 protein expression in dose and time studies, though the effect was reverted at 100 nM of both compounds. Moreover, A20 mRNA was rapidly decreased at 3 h and sustained up to 72 h (Fig. 5B); response that was reflected in a decrement in A20 protein expression (12–72 h) analyzed by Western blot (Fig. 5C). In addition, this effect was found to be VDR dependent (Fig. 7).

3.6. 1α,25(OH)$_2$D$_3$ or TX 527 induces changes in BECN1 expression

BECN1 is a protein that is expressed in many human tissues and there is evidence suggesting that the transcription factor E2F and NF-κB are involved in the regulation of its expression [48]. Wang and colleagues demonstrated that 1α,25(OH)$_2$D$_3$ induces autophagy in human myeloid leukemia cells by up-regulation of BECN1 expression and inhibition of mTOR phosphorylation [37]. We next evaluated whether BECN1 is regulated by both VDR agonists. First, vGPCR cells were treated with 10 nM of 1α,25(OH)$_2$D$_3$ or TX 527 or vehicle (0.01% ethanol) at different times (Fig. 8). BECN1 mRNA levels were analyzed in time-response studies (6–48 h) by qRT-PCR (Fig. 8A). Treatment with 1α,25(OH)$_2$D$_3$ caused a significant decrease in BECN1 mRNA levels at 12 and 24 h, whereas at 48 h, a highly significant increase was observed. In contrast, TX 527 caused a significant increase in BECN1 mRNA levels at 12 and 24 h, and a highly significant decrease at 48 h. Secondly; we investigated whether changes in BECN1 mRNA expression were reflected into changes in its protein levels in parallel experiments (Fig. 8B). The quantification of the results obtained reveal that 1α,25(OH)$_2$D$_3$ induced a significant increase in BECN1 protein levels at 24 h and a decrease at 12 and 48 h; meanwhile, TX 527 induced a significant increase in BECN1 in a time dependent manner between 12 to 48 h. Discrepancies observed between transcript and protein levels at same time point could be related with regulatory mechanisms occurring after mRNA is synthetized and protein abundance regulation.

3.7. 1α,25(OH)$_2$D$_3$ or TX 527 inhibits mTOR phosphorylation and induces autophagy by a PI3K/Akt dependent mechanism

As outlined in the introduction, autophagy is governed by a series of Atg genes, being LC3 an important biomarker of autophagy. During the process of autophagosome development, ATG8 proteins are specifically cleaved to expose a glycine residue to become 'form I' proteins, then, this glycine residue is then conjugated to phosphatidylethanolamine, changing into 'form II' proteins [23]. Fleet and collaborators reported that 1α,25(OH)$_2$D$_3$ suppresses mTOR in leukemia cells contributing to the development of autophagy [49]. Next, mTOR phosphorylation status was evaluated as a measure of its activity and LC3-II proteins levels as a measure of autophagy. vGPCR cells were treated with 10 nM of 1α,25(OH)$_2$D$_3$ or TX 527 or vehicle (0.01% ethanol) for 48 h (Fig. 9A). To evaluate the participation of the PI3K/Akt/mTOR axis in autophagy triggered by 1α,25(OH)$_2$D$_3$, vGPCR cells were incubated with 10 μM of LY294002 or vehicle (0.01% ethanol) during 15 min prior to 1α,

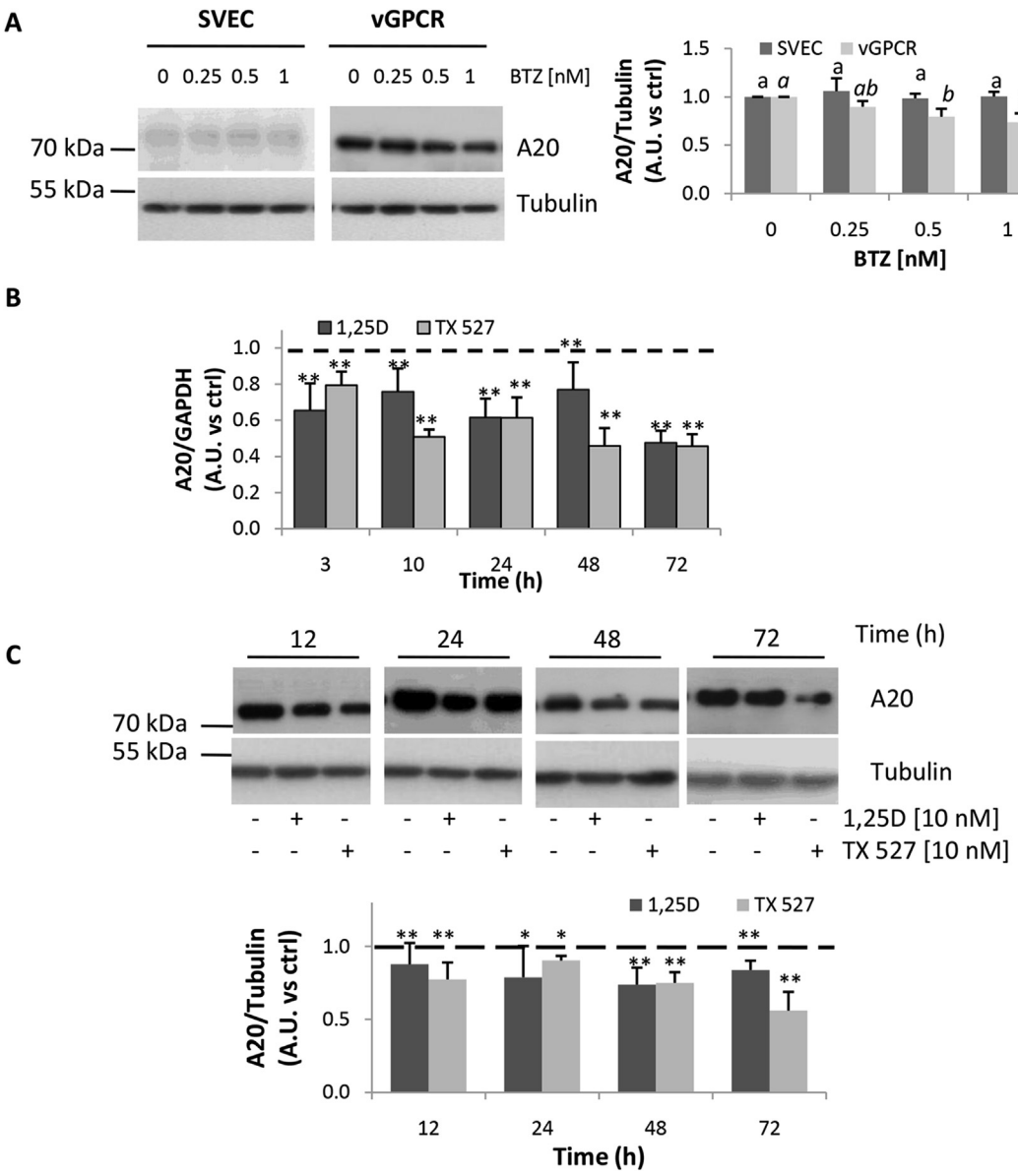

Fig. 5. A20 is regulated by Bortezomib and VDR agonists in vGPCR cells. A) SVEC and vGPCR cells were treated with Bortezomib (0.25–1 nM) or vehicle (DMSO, 0.1%) for 24 h A20 protein levels were tested by Western blot and Tubulin was used as loading control. Representative blots of at least three independent experiments and their quantification plotted on a bar graph are shown. The statistical differences were analyzed by one-way ANOVA followed by the Bonferroni test. Different letters indicate significant differences ($p < 0.05$). vGPCR cells were treated with 10 nM of $1\alpha,25(OH)_2D_3$ (1,25D) or TX 527 or vehicle (0.01% ethanol) at different times to evaluate A20 gene (3–72 h) and protein (12–72 h) expression. B) Total RNA was isolated and A20 expression was evaluated on the resulting cDNA and the values obtained were normalized with GAPDH as shown in the bar graph. C) Protein levels of A20 and Tubulin were analyzed by Western blot. Representative blots and their quantification of at least three independent experiments are shown in a bar graph. Significant differences between 1,25D or TX527 and their respective control at each time were analyzed by the Student's t test (*$p < 0.05$, **$p < 0.01$). Full, non-adjusted and uncropped images are shown in suppl. Material.

$25(OH)_2D_3$ treatment (10 nM) or vehicle (0.01% ethanol) for 48 h (Fig. 9B). The results shown in Fig. 9A indicate that $1\alpha,25(OH)_2D_3$ or TX 527 decreased mTOR phosphorylation without causing changes in its total protein levels. In addition, autophagy was induced by $1\alpha,25(OH)_2D_3$ (Fig. 9B) and in presence of LY294002, LC3-II levels were significant increased comparable to $1\alpha,25(OH)_2D_3$ treatment. Moreover, LC3-II levels showed no greater increase when LY294002 was combined with $1\alpha,25(OH)_2D_3$.

3.8. Inhibition of autophagy flow with Chloroquine induces LC3 proteins levels like VDR agonists

Because the accumulation of autophagosomes is toxic to cells [50, 51], the blockage of autophagosomes degradation with Chloroquine after $1\alpha,25(OH)_2D_3$ or TX 527 treatment could be detrimental to vGPCR cells survival and this would allow us to confirm autophagy induction. To test this hypothesis, vGPCR cells were treated with 10 nM of $1\alpha,25(OH)_2D_3$ or TX 527 or vehicle (0.01% of ethanol) for 48 h and 30 min prior to finish VDR agonists treatments, Chloroquine (1 μM, CQ) was added to inhibit autophagy flow by decreasing the autophagosome-lysosome fusion [52, 53, 54]. In presence of CQ, LC3-II levels were comparable to control condition and in combination with $1\alpha,25(OH)_2D_3$ did not increase, whereas with TX 527 the effect observed was enhanced (Fig. 10A). We also investigated whether VDR participates in LC3-II induction by both VDR agonists. For this, vGPCR-shVDR or vGPCR-shctrl cells were treated with 10 nM of $1\alpha,25(OH)_2D_3$ or TX 527 or vehicle (0.01% ethanol) for 48

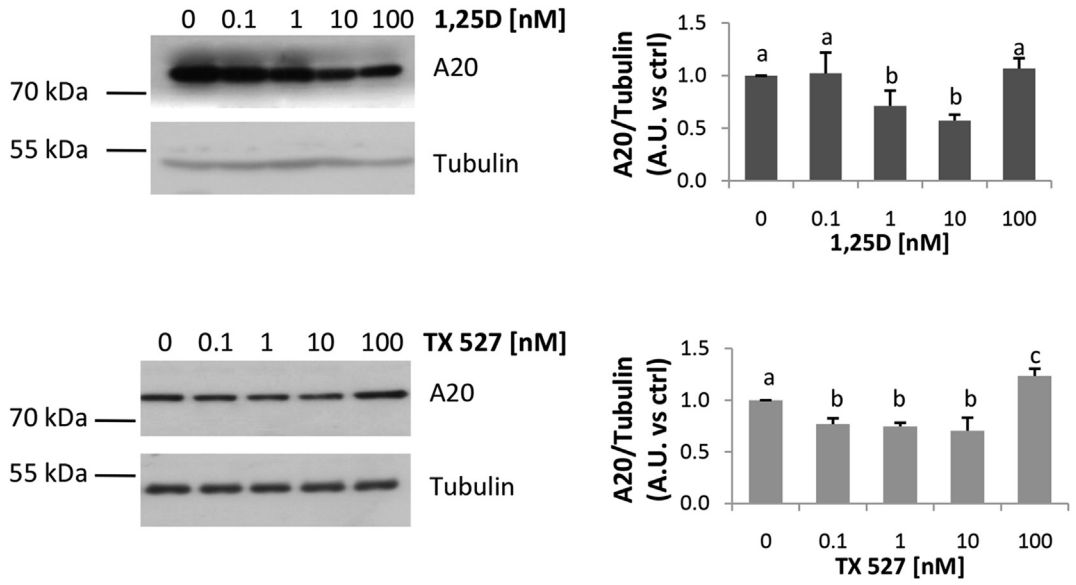

Fig. 6. 1α,25(OH)$_2$D$_3$ or TX 527 decreased A20 protein levels in a dose dependent manner in vGPCR cells. vGPCR cells were treated with increasing concentrations of 1α,25(OH)$_2$D$_3$ or TX 527 (0–100 nM) or vehicle (0.01 % ethanol) for 48 h. Cell lysates were subject to Western blot analysis with anti-A20 and anti-Tubulin antibodies. Representative blots and quantification of at least three independent experiments are shown. Full, non-adjusted and uncropped images are shown in suppl. Material. Protein bands quantification were achieved by densitometry and then represented in bar graphs as the radio between A20 and Tubulin referred to vehicle. The statistical analysis of the results was carried out by one way-ANOVA followed by Bonferroni test. Different letters indicate statistical significances at *p < 0.01.

h (Fig. 10B). The results showed that the significant increase in LC3-II amount was suppressed when VDR expression was knockdown indicating that both, 1α,25(OH)$_2$D$_3$ and TX 527, exert their actions through a VDR dependent mechanism of action.

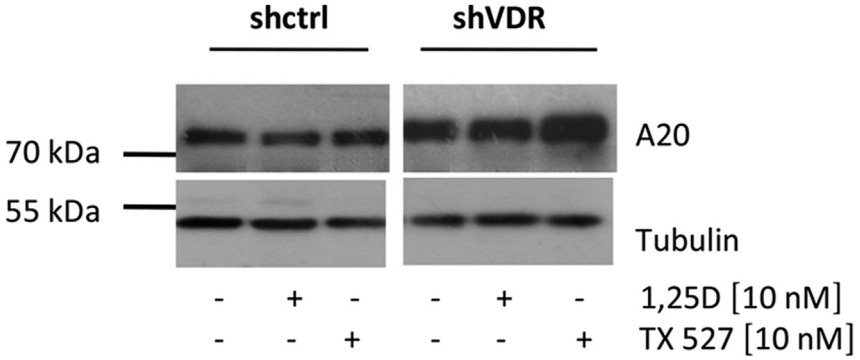

Fig. 7. A20 downregulation by VDR agonists is VDR dependent. Stable vGPCR cells targeted with small hairpin RNA against mouse VDR (vGPCR-shVDR) or control (vGPCR-shctrl) were treated with 10 nM of 1α,25(OH)$_2$D$_3$ or TX 527 or vehicle (0.01% ethanol) for 48 h. Total protein from cells lysates were subject to Western blot analysis with anti-A20 and anti-Tubulin antibodies. A representative Western blot from four independent experiments is shown; full, non-adjusted and uncropped images are shown in suppl. Material. A20 protein bands were quantified, normalized using Tubulin, and represented in a bar graph. Significant differences between control (vehicle) and stimulated cells were analyzed by one-way ANOVA followed by Bonferroni test, p < 0.01.

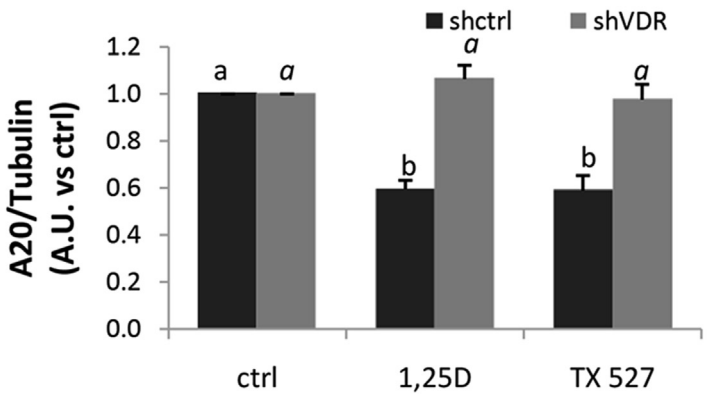

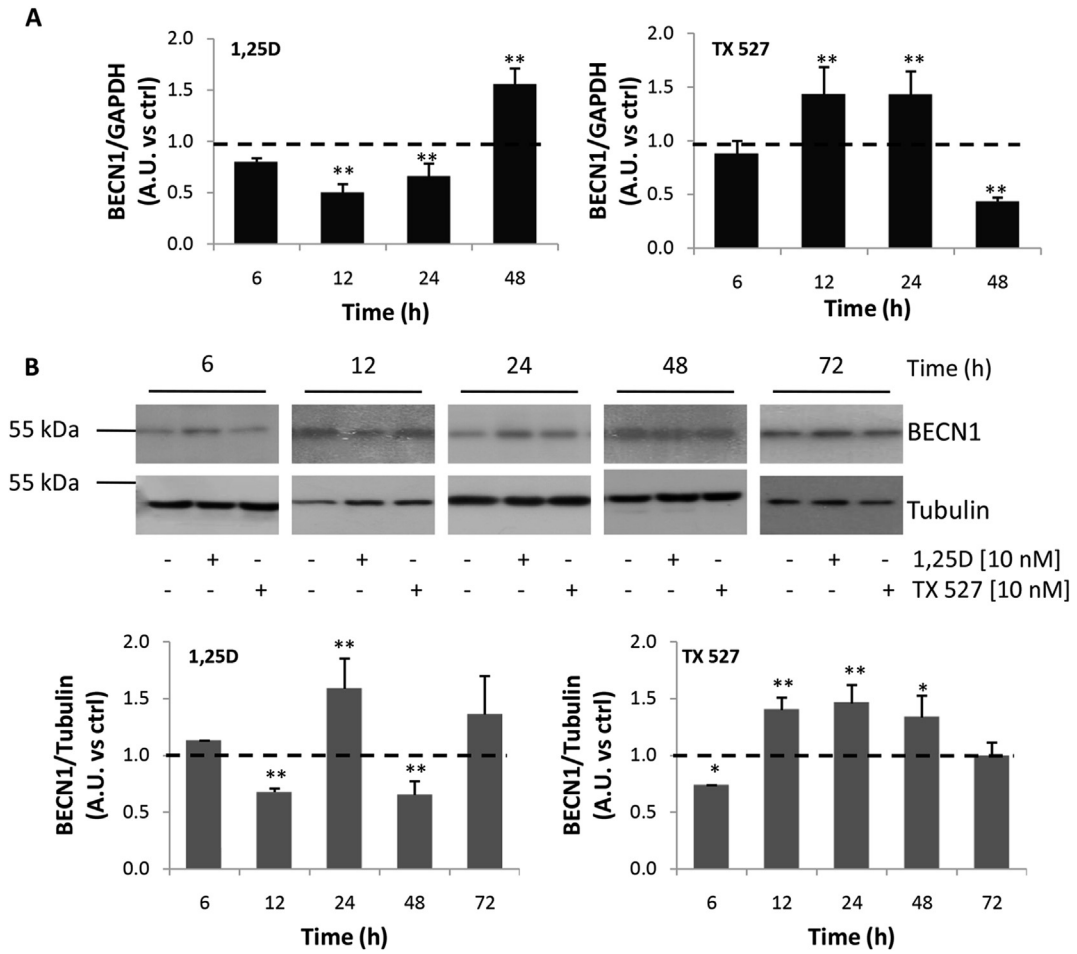

Fig. 8. 1α,25(OH)$_2$D$_3$ or TX 527 induces changes in BECN1 expression. vGPCR cells were treated with 10 nM of 1α,25(OH)$_2$D$_3$ (1,25D) or TX 527 or vehicle (0.01% ethanol) for different times to evaluate BECN1 gene (6–48 h) and protein (6–72 h) expression. A) Total RNA was isolated and BECN1 expression was evaluated on the resulting cDNA and the values obtained were normalized with GAPDH as shown in the bar graph. B) Protein levels of BECN1 and Tubulin were analyzed by Western blot. Representative blots and their quantification of at least three independent experiments are shown in a bar graph; full, non-adjusted and uncropped images are shown in suppl. Material. Significant differences between 1,25D or TX527 and their respective control at each time were analyzed by Student's t test (*$p < 0.05$, **$p < 0.01$).

4. Discussion

Apoptosis and autophagy are evolutionarily conserved processes that regulate cell fate. Both processes are important for the development and normal physiology of tissues and have been found to be regulated in a wide range of diseases [55]. It is well known that infection with KSHV induces the expression of viral proteins that contribute to the development of different malignancies. It has been observed that vFLIP, for example, suppresses apoptosis and autophagy favoring cell survival. On the other hand, infection with KSHV activates mTOR, a negative regulator of autophagy process and an important molecule for cell proliferation, modulation and angiogenesis [5]. Autophagy is induced by several forms of cellular stress including starvation, hypoxia and infection, as well as can be induced by drugs used in therapy against cancer and other diseases [44, 56]. Numerous studies have shown that 1α,25(OH)$_2$D$_3$ has the ability to induce autophagy in different cell types. For instance, in lymphoma cells and breast cancer, 1α,25(OH)$_2$D$_3$ and its analog EB1089 showed a cytotoxic effect triggering cell death by a caspase independent mechanism, characterized by an increase in lysosomal activity [38]. In addition, 1α,25(OH)$_2$D$_3$ has shown to induce autophagy in myeloid leukemia and in luminal breast cancer cells [37, 39]. Also, 1α,25(OH)$_2$D$_3$-induced autophagy may require a complex interplay with CDK inhibitors, for instance, in p19 deficient SCC25 cells 1α,25(OH)$_2$D$_3$ autophagy induction can be suppressed by p27 suppression [57]. Moreover, studies in breast cancer cells revealed that the combined treatment of 1α,25(OH)$_2$D$_3$ plus ionizing radiation induces cytotoxic autophagy [58]. This effect of 1α,25(OH)$_2$D$_3$ is not limited to cancer cells. In this regard, concentrations at picomolar order of the metabolite have shown to induce autophagy in primary monocytes and macrophages suggesting that it could stimulate autophagy in normal physiological conditions [59]. 1α,25(OH)$_2$D$_3$ may prevent human umbilical vein endothelial cells death through modulation of the interplay between apoptosis and autophagy. This effect is obtained by inhibiting superoxide anion generation, maintaining mitochondria function and cell viability, activating survival kinases, and inducing nitric oxide production [60]. In this work, we have obtained evidence indicating that inhibition of PI3K/Akt pathway causes a decrease in cell proliferation comparable to VDR agonists in vGPCR cells. As previously mentioned, Akt plays a crucial role in the development of KS [7, 11]. Moreover, we found that both VDR agonists reduce Akt phosphorylation state through a VDR dependent mechanism and decreases its translocation to the nucleus. In support of these results, recent findings *in vitro* and *in vivo* studies in breast cancer models showed an active role of 1α,25(OH)$_2$D$_3$ in the induction of autophagy by a mechanism that involves VDR participation [39]. Wu and colleagues demonstrated that the absence of intestinal epithelial VDR affects microbial assemblage and increases susceptibility to dextran sulfate

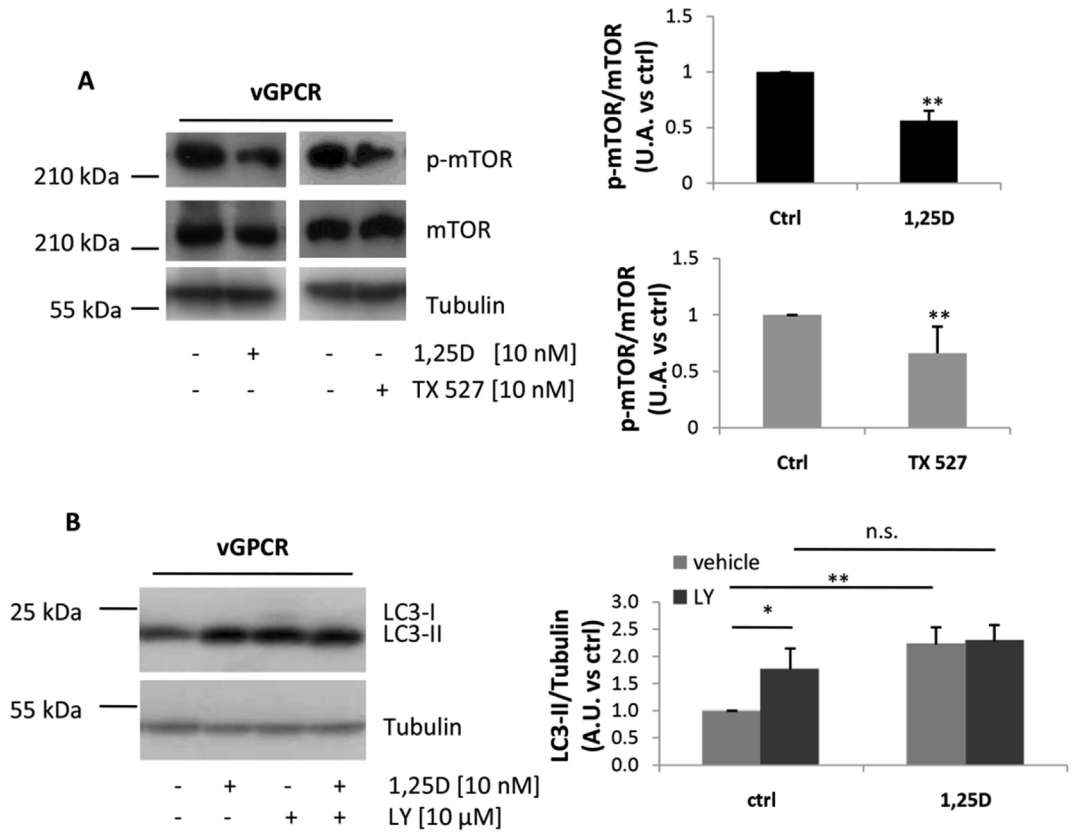

Fig. 9. 1α,25(OH)$_2$D$_3$ or TX 527 decreases mTOR phosphorylation and induces autophagy. vGPCR cells were incubated with 10 μM of LY294002 (LY) or vehicle (0.01% ethanol) for 15 min prior to 1α,25(OH)$_2$D$_3$ (10 nM) or vehicle (0.01% ethanol). The protein levels of phosphorylated and total mTOR (A) or LC3 (B) were analyzed by Western blot using Tubulin as loading control. Representative blots are shown and the quantification of six independent experiments is represented in bar graphs. Significant differences between conditions were evaluated in A) by one-way ANOVA followed by the Bonferroni test ($p < 0.05$) or B) significant differences between pairs of conditions were evaluated through the Student t test (*$p < 0.05$, **$p < 0.01$, n. s: not significant). Full, non-adjusted and uncropped images are shown in suppl. Material.

sodium-induced colitis. Also, VDR down regulates ATG16L1 and lysozyme expression, and impairs antimicrobial function and autophagy of Paneth cells [61]. Similar to VDR agonists, Bortezomib caused a decrease in Akt phosphorylation in a dose-dependent manner. In support of this result, studies in different hepatocarcinoma cell lines showed that Bortezomib decreases Akt phosphorylation/activation preceding cell death by apoptosis [62]. Furthermore, in SK-BR-3 cells, a marked inhibition of EGFR, HER-2, and Akt phosphorylation was observed at a clinically relevant concentration of Bortezomib [63]. In this work, we have also obtained evidence that 1α,25(OH)$_2$D$_3$ or TX 527 decreased mTOR phosphorylation and induced autophagy revealed by an increment in LC3-II marker, an event that is triggered by inactivation of PI3K/Akt pathway. In agreement with this result, *in vivo* studies showed that treatment with Hesperidin attenuates myocardial lesions caused by ischemia/reperfusion by suppressing autophagy through activation of the PI3K/Akt/mTOR pathway [64]. Also, Yang and collaborators presented data suggesting that the protective role of vitamin D in mouse liver ischemia/reperfusion injury is autophagy-dependent, which is regulated by both MEK/ERK and PTEN/PI3K/Akt/mTOR pathway [65].

Many autophagy regulators are substrates for ubiquitin E3 ligases or deubiquitinating enzymes, therefore ubiquitination modifications of these autophagy regulators result in autophagy induction or termination [66]. As was mentioned before, TNFAIP3/A20 is a direct NF-κB target gene, and A20 expression could limit autophagy by regulating BECN1. We have found that A20 is highly expressed in vGPCR and its expression is down-regulated by the inhibition of NF-κB with Bortezomib or VDR agonists in a VDR dependent manner. We have also found that BECN1 is temporarily modulated by VDR agonists. Although BECN1 mRNA and protein levels vary, when it is increased, it would regulate the initial steps of autophagy. Autophagy and apoptosis can be trigger by common stimuli and signaling pathways leading to a balance between both processes. It has been described that BECN1 is involved in these processes. On one hand, BECN1 participates in autophagosome formation upon autophagy stimuli, on the other, it can be cleaved by caspases, translocate to the mitochondria, and participate in apoptosis induction [48]. We have shown in previous studies that apoptosis is induced by VDR agonists by a caspase-3 dependent mechanism in vGPCR cells [35], so that, the differences observed in BECN1 levels could be explained by the fact that this protein could cooperate in both processes to contribute to cell death. In support of our results, BECN1has shown to participate in the activation of apoptosis and autophagy pathways induced by EB1089, a synthetic analog of 1α,25(OH)$_2$D$_3$, in breast cancer cells (MCF-7) [67]. On the other hand, an increase in BECN1 levels, triggers differentiation, inhibits apoptosis and induces autophagy in myeloid leukemia cells after 1α, 25(OH)$_2$D$_3$ treatment [37].

5. Conclusions

Taken together, these results demonstrate that 1α,25(OH)$_2$D$_3$ or TX 527 induces autophagy in endothelial cells expressing vGPCR through the inactivation of PI3K/Akt/mTOR axis by a VDR-dependent mechanism.

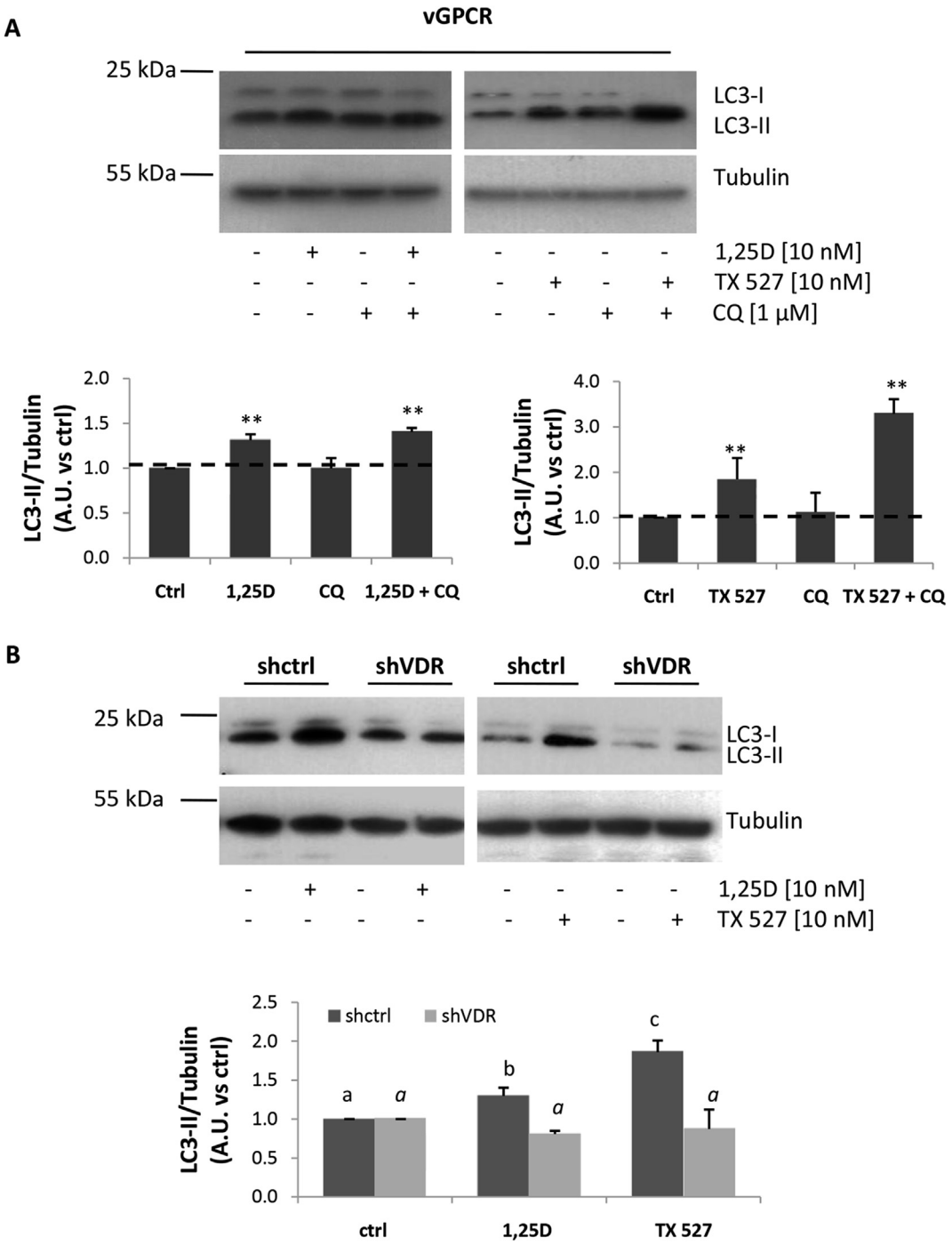

Fig. 10. Inhibition of autophagy flow with Chloroquine induces LC3 levels and is VDR dependent. A) Cells were treated with 10 nM of 1α,25$(OH)_2D_3$ (1,25D) or TX 527 or vehicle (0.01% of ethanol) for 48 h and 30 min before the end of VDR agonists treatments, 1 μM of Chloroquine (CQ) was added. B) vGPCR-shctrl (shctrl) and vGPCR-shVDR (shVDR) cells were cultured and treated with 10 nM of 1α,25$(OH)_2D_3$ (1,25D) or TX 527 or vehicle (0.01% ethanol) for 48 h LC3 and Tubulin levels were evaluated by Western blot. A representative blot of three independent experiments is shown, and the quantification is represented in bar graphs. Full, non-adjusted and uncropped images are shown in suppl. Material. In A) significant differences between conditions were evaluated by Student's t test between 1,25D or TX 527 or CQ and ctrl (*$p < 0.05$, **$p < 0.01$) whereas in B) significant differences between control (vehicle) and agonists were analyzed by one-way ANOVA, followed by the Bonferroni test. Significant differences between conditions are indicated by different letters ($p < 0.05$).

Declarations

Author contribution statement

Alejanadra Suares: Conceived and designed the experiments; Performed the experiments; Analyzed and interpreted the data.

Cinthya Tapia: Performed the experiments.

Veronica Gonzalez Pardo: Conceived and designed the experiments; Analyzed and interpreted the data; Contributed reagents, materials, analysis tools or data; Wrote the paper.

Funding statement

This work was supported by grants from Agencia Nacional de

Promoción Científica y Tecnológica (PICT 2013–0562), Consejo Nacional de Investigaciones Científicas y Tecnológicas (CONICET, PIP1122011010040) and Universidad Nacional del Sur (PGI 24/ZB68) to Verónica González Pardo.

Competing interest statement

The authors declare no conflict of interest.

Additional information

Supplementary content related to this article has been published online at https://doi.org/10.1016/j.heliyon.2019.e02367.

Acknowledgements

We wish to thank Dr. Daniel Grasso (IBIMOL Universidad de Buenos Aires – CONICET) for providing the inhibitor of flux autophagy, Chloroquine.

References

[1] M. Angelova, M. Ferris, K.F. Swan, H.E. McFerrin, G. Pridjian, C.A. Morris, et al., Kaposi's sarcoma-associated herpesvirus G-protein coupled receptor activates the canonical Wnt/β-catenin signaling pathway, Virol. J. 11 (2014) 218.
[2] T.F. Schulz, E. Cesarman, Kaposi sarcoma-associated herpesvirus: mechanisms of oncogenesis, Curr. Opin. Virol. 14 (2015) 116–128.
[3] S. Montaner, A. Sodhi, A. Molinolo, T.H. Bugge, E.T. Sawai, Y. He, et al., Endothelial infection with KSHV genes in vivo reveals that vGPCR initiates Kaposi's sarcomagenesis and can promote the tumorigenic potential of viral latent genes, Cancer Cell 3 (2003) 23–36.
[4] D. Martin, J.S. Gutkind, Human tumor-associated viruses and new insights into the molecular mechanisms of cancer, Oncogene 27 (2008) S31–42.
[5] E.A. Mesri, E. Cesarman, C. Boshoff, Kaposi's sarcoma and its associated herpesvirus, Nat. Rev. Cancer 10 (2010) 707–719.
[6] K.J. Zwezdaryk, J.A. Combs, C.A. Morris, D.E. Sullivan, Regulation of Wnt/β-catenin signaling by herpesviruses, World J. Virol. 5 (2016) 144.
[7] A. Sodhi, R. Chaisuparat, J. Hu, A.K. Ramsdell, B.D. Manning, E.A. Sausville, et al., The TSC2/mTOR pathway drives endothelial cell transformation induced by the Kaposi's sarcoma-associated herpesvirus G protein-coupled receptor, Cancer Cell 10 (2006) 133–143.
[8] C. Bais, B. Santomasso, O. Coso, L. Arvanitakis, E.G. Raaka, J.S. Gutkind, et al., G-protein-coupled receptor of Kaposi's sarcoma-associated herpesvirusis a viral oncogene and angiogenesis activator, Nature 391 (1998) 86–89.
[9] D. Martin, R. Galisteo, J.S. Gutkind, CXCL8/IL8 stimulates vascular endothelial growth factor (VEGF) expression and the autocrine activation of VEGFR2 in endothelial cells by activating NFκB through the CBM (Carma3/Bcl10/Malt1) complex, J. Biol. Chem. 284 (2009) 6038–6042.
[10] M.M. Rosenkilde, T.N. Kledal, P.J. Holst, T.W. Schwartz, Selective elimination of high constitutive activity or chemokine binding in the human herpesvirus 8 encoded seven transmembrane oncogene ORF74, J. Biol. Chem. 275 (2000) 26309–26315.
[11] A. Sodhi, S. Montaner, V. Patel, J.J. Gómez-Román, Y. Li, E.A. Sausville, et al., Akt plays a central role in sarcomagenesis induced by Kaposi's sarcoma herpesvirus-encoded G protein-coupled receptor, Proc. Natl. Acad. Sci. U. S. A. 101 (2004) 4821–4826.
[12] C. Bais, A. Van Geelen, P. Eroles, A. Mutlu, C. Chiozzini, S. Dias, et al., Kaposi's sarcoma associated herpesvirus G protein-coupled receptor immortalizes human endothelial cells by activation of the VEGF receptor-2/KDR, Cancer Cell 3 (2003) 131–143.
[13] D. Martin, R. Galisteo, A.A. Molinolo, R. Wetzker, E. Hirsch, J.S. Gutkind, Report PI3K g mediates kaposi ' s sarcoma-associated herpesvirus vGPCR- induced sarcomagenesis, Cancer Cell 19 (2011) 805–813.
[14] M.P. Wymann, M. Zvelebil, M. Laffargue, Phosphoinositide 3-kinase signalling - which way to target? Trends Pharmacol. Sci. 24 (2003) 366–376.
[15] R. Courtnay, D.C. Ngo, N. Malik, K. Ververis, S.M. Tortorella, T.C. Karagiannis, Cancer metabolism and the Warburg effect: the role of HIF-1 and PI3K, Mol. Biol. Rep. 42 (2015) 841–851.
[16] X. Shao, D. Lai, L. Zhang, H. Xu, Induction of autophagy and apoptosis via PI3K/AKT/TOR pathways by azadirachtin a in spodoptera litura cells, Sci. Rep. 6 (2016) 1–12.
[17] C. He, D.J. Klionsky, Regulation mechanisms and signaling pathways of autophagy, Annu. Rev. Genet. 43 (2009) 67–93.
[18] L. Galluzzi, F. Pietrocola, J.M. Bravo-San Pedro, R.K. Amaravadi, E.H. Baehrecke, F. Cecconi, et al., Autophagy in malignant transformation and cancer progression, EMBO J. 34 (2015) 856–880.
[19] M.I. Vaccaro, Autophagy, physiology and cell pathology, Physiol. Mini Rev. 6 (2013).
[20] K. Inoki, J. Kim, K.-L. Guan, AMPK and mTOR in cellular energy homeostasis and drug targets, Annu. Rev. Pharmacol. Toxicol. 52 (2012) 381–400.
[21] M. Laplante, D.M. Sabatini, mTOR signaling in growth control and disease, Cell 149 (2012) 274–293.
[22] F. Nazio, F. Strappazzon, M. Antonioli, P. Bielli, V. Cianfanelli, M. Bordi, et al., mTOR inhibits autophagy by controlling ULK1 ubiquitylation, self-association and function through AMBRA1 and TRAF6, Nat. Cell Biol. 15 (2013) 406–416.
[23] T. Into, M. Inomata, E. Takayama, T. Takigawa, Autophagy in regulation of Toll-like receptor signaling, Cell. Signal. 24 (2012) 1150–1162.
[24] Y. Kabeya, N. Mizushima, T. Ueno, A. Yamamoto, T. Kirisako, T. Noda, et al., Erratum: LC3, a mammalian homolog of yeast Apg8p, is localized in autophagosome membranes after processing (EMBO Journal (2000) 19 (5720-5728, EMBO J. 22 (2003) 4577.
[25] M.R. Haussler, G.K. Whitfield, I. Kaneko, C.A. Haussler, D. Hsieh, J.-C. Hsieh, et al., Molecular mechanisms of vitamin D action, Calcif. Tissue Int. 92 (2013) 77–98.
[26] A.V. Krishnan, D.L. Trump, C.S. Johnson, D. Feldman, The role of vitamin D in cancer prevention and treatment, Rheum. Dis. Clin. N. Am. 38 (2012) 161–178.
[27] A.V. Krishnan, D. Feldman, Mechanisms of the anti-cancer and anti-inflammatory actions of vitamin D, Annu. Rev. Pharmacol. Toxicol. 51 (2011) 311–336.
[28] K.K. Deeb, D.L. Trump, C.S. Johnson, Vitamin D signalling pathways in cancer: potential for anticancer therapeutics, Nat. Rev. Cancer 7 (2007) 684–700.
[29] L. Díaz, M. Díaz-Muñoz, A. García-Gaytán, I. Méndez, Mechanistic effects of calcitriol in cancer biology, Nutrients 7 (2015) 5020–5050.
[30] J. Welsh, Vitamin D and prevention of breast cancer, Acta Pharmacol. Sin. 28 (9) (2007 Sep) 1373–1382. Review.
[31] D. Feldman, A.V. Krishnan, S. Swami, E. Giovannucci, B.J. Feldman, The role of vitamin D in reducing cancer risk and progression, Nat. Rev. Cancer 14 (2014) 342–357.
[32] V. Gonzalez-Pardo, D. Martin, J.S. Gutkind, A. Verstuyf, R. Bouillon, A.R. de Boland, et al., 1α,25-Dihydroxyvitamin D 3 and its TX527 analog inhibit the growth of endothelial cells transformed by kaposi sarcoma-associated herpes virus G protein-coupled receptor in vitro and in vivo, Endocrinology 151 (2010) 23–31.
[33] V. Gonzalez-Pardo, N. D'Elia, A. Verstuyf, R. Boland, A. Russo de Boland, NFκB pathway is down-regulated by 1α,25(OH)(2)-vitamin D(3) in endothelial cells transformed by Kaposi sarcoma-associated herpes virus G protein coupled receptor, Steroids 77 (2012) 1025–1032.
[34] V. González-Pardo, A. Verstuyf, R. Boland, A. Russo de Boland, Vitamin D analogue TX 527 down-regulates the NF-κB pathway and controls the proliferation of endothelial cells transformed by Kaposi sarcoma herpesvirus, Br. J. Pharmacol. 169 (2013) 1635–1645.
[35] V. González-Pardo, A. Suares, A. Verstuyf, P. De Clercq, R. Boland, A.R. de Boland, Cell cycle arrest and apoptosis induced by 1α,25(OH)2D3 and TX 527 in Kaposi sarcoma is VDR dependent, J. Steroid Biochem. Mol. Biol. 144 (2014) 197–200.
[36] A. Suares, A. Russo de Boland, A. Verstuyf, R. Boland, V. González-Pardo, The proapoptotic protein Bim is up regulated by 1α,25-dihydroxyvitamin D3 and its receptor agonist in endothelial cells and transformed by viral GPCR associated to Kaposi sarcoma, Steroids 102 (2015) 85–91.
[37] J. Wang, H. Lian, Y. Zhao, M.A. Kauss, S. Spindel, Vitamin D3 induces autophagy of human myeloid leukemia, Cells 283 (2008) 25596–25605.
[38] M. Høyer-Hansen, S.P.S. Nordbrandt, M. Jäättelä, Autophagy as a basis for the health-promoting effects of vitamin D, Trends Mol. Med. 16 (2010) 295–302.
[39] L.E. Tavera-Mendoza, T. Westerling, E. Libby, A. Marusyk, L. Cato, R. Cassani, et al., Vitamin D receptor regulates autophagy in the normal mammary gland and in luminal breast cancer cells, Proc. Natl. Acad. Sci. 114 (2017) E2186–E2194.
[40] W. Strober, Trypan blue exclusion test of cell viability, Hoboken, NJ, USA: John Wiley & Sons, Inc. Curr. Protoc. Im. 111 (2001). A3.B.1-A3.B.3
[41] V.G. Pardo, R. Boland, A.R. de Boland, 1α,25(OH)2-Vitamin D3 stimulates intestinal cell p38 MAPK activity and increases c-Fos expression, Int. J. Biochem. Cell Biol. 38 (2006) 1181–1190.
[42] V. González Pardo, R. Boland, A.R. de Boland, Vitamin D receptor levels and binding are reduced in aged rat intestinal subcellular fractions, Biogerontology 9 (2008) 109–118.
[43] A. Suares, M. Mori Sequeiros Garcia, C. Paz, V. González-Pardo, Antiproliferative effects of Bortezomib in endothelial cells transformed by viral G protein-coupled receptor associated to Kaposi's sarcoma, Cell. Signal. 32 (2017) 124–132.
[44] D. Martin, R. Galisteo, A.A. Molinolo, R. Wetzker, E. Hirsch, J.S. Gutkind, PI3Kγ mediates kaposi's sarcoma-associated herpesvirus vGPCR-induced sarcomagenesis, Cancer Cell 19 (2011) 805–813.
[45] A.W. Norman, From vitamin D to hormone D: fundamentals of the vitamin D endocrine system essential for good health, Am. J. Clin. Nutr. 88 (2008) 491S–499S.
[46] Y. Matsuzawa, S. Oshima, M. Takahara, C. Maeyashiki, Y. Nemoto, M. Kobayashi, et al., TNFAIP3 promotes survival of CD4 T cells by restricting MTOR and promoting autophagy, Autophagy 11 (2015) 1052–1062.
[47] C.-S. Shi, J.H. Kehrl, TRAF6 and A20 regulate lysine 63-linked ubiquitination of Beclin-1 to control TLR4-induced autophagy, Sci. Signal. 3 (2010) ra42.
[48] R. Kang, H.J. Zeh, M.T. Lotze, D. Tang, The Beclin 1 network regulates autophagy and apoptosis, Cell Death Differ. 18 (2011) 571–580.
[49] J.C. Fleet, M. DeSmet, R. Johnson, Y. Li, Vitamin D and cancer: a review of molecular mechanisms, Biochem. J. 441 (2012) 61–76.
[50] J. Fields, W. Dumaop, S. Eleuteri, S. Elueteri, S. Campos, E. Serger, et al., HIV-1 Tat alters neuronal autophagy by modulating autophagosome fusion to the lysosome:

implications for HIV-associated neurocognitive disorders, J. Neurosci. 35 (2015) 1921–1938.
[51] S. Khoh-Reiter, S.A. Sokolowski, B. Jessen, M. Evans, D. Dalvie, S. Lu, Contribution of membrane trafficking perturbation to retinal toxicity, Toxicol. Sci. 145 (2015) 383–395.
[52] M. Mauthe, I. Orhon, C. Rocchi, X. Zhou, M. Luhr, K.-J. Hijlkema, et al., Chloroquine inhibits autophagic flux by decreasing autophagosome-lysosome fusion, Autophagy 14 (2018) 1435–1455.
[53] D. Grasso, A. Ropolo, Re A. Lo, J.L. Iovanna, C.D. Gonzalez, M.I. Vaccaro, Zymophagy , a novel selective autophagy pathway mediated by VMP1-USP9x-p62, Prev. Pancreat. Cell Death 286 (2011) 8308–8324.
[54] D.S. Ojeda, D. Grasso, J. Urquiza, A. Till, M.I. Vaccaro, J. Quarleri, Cell death is counteracted by mitophagy in HIV-productively infected astrocytes but is promoted by inflammasome activation among non-productively, Infected Cells 9 (2018) 1–19.
[55] A. Thorburn, Apoptosis and autophagy: regulatory connections between two supposedly different processes, Apoptosis 13 (2008) 1–9.
[56] M. Høyer-Hansen, M. Jäättelä, Autophagy: an emerging target for cancer therapy, Autophagy 4 (2008) 574–580.
[57] L. Tavera-Mendoza, T.-T. Wang, B. Lallemant, R. Zhang, Y. Nagai, V. Bourdeau, et al., Convergence of vitamin D and retinoic acid signalling at a common hormone response element, EMBO Rep. 7 (2006) 180–185.
[58] E.N. Wilson, M.L. Bristol, X. Di, W.A. Maltese, K. Koterba, M.J. Beckman, et al., A switch between cytoprotective and cytotoxic autophagy in the radiosensitization of breast tumor cells by chloroquine and vitamin D, Horm Cancer 2 (2011) 272–285.
[59] M. Fabri, R.L. Modlin, A vitamin for autophagy, Cell Host Microbe 6 (2009) 201–203.
[60] F. Uberti, D. Lattuada, V. Morsanuto, U. Nava, G. Bolis, G. Vacca, et al., Vitamin D protects human endothelial cells from oxidative stress through the autophagic and survival pathways, J. Clin. Endocrinol. Metab. 99 (2014) 1367–1374.
[61] S. Wu, Y. Zhang, R. Lu, Y. Xia, D. Zhou, E.O. Petrof, et al., Intestinal epithelial vitamin D receptor deletion leads to defective autophagy in colitis, Gut 64 (2015) 1082–1094.
[62] K.-F. Chen, P.-Y. Yeh, K.-H. Yeh, Y.-S. Lu, S.-Y. Huang, A.-L. Cheng, Down-regulation of phospho-akt is a major molecular determinant of bortezomib-induced apoptosis in hepatocellular carcinoma cells, Cancer Res. 68 (2008) 6698–6707.
[63] J. Codony-Servat, M.A. Tapia, M. Bosch, C. Oliva, J. Domingo-Domenech, B. Mellado, et al., Differential cellular and molecular effects of bortezomib, a proteasome inhibitor, in human breast cancer cells, Mol. Cancer Ther. 5 (2006) 665–675.
[64] X. Li, X. Hu, J. Wang, W. Xu, C. Yi, R. Ma, et al., Inhibition of autophagy via activation of PI3K/Akt/mTOR pathway contributes to the protection of hesperidin against myocardial ischemia/reperfusion injury, Int. J. Mol. Med. (2018) 1917–1924.
[65] J.H. Yang, Q. Chen, S.Y. Tian, S.H. Song, F. Liu, Q.X. Wang, et al., The role of 1,25-dyhydroxyvitamin D3in mouse liver ischemia reperfusion injury: regulation of autophagy through activation of mek/erk signaling and pten/pi3k/akt/mtorc1 signaling, Am. J. Transl. Res. 7 (2015) 2630–2645.
[66] K. Zientara-rytter, S. Subramani, The roles of ubiquitin-binding protein shuttles in the degradative fate of ubiquitinated proteins in the ubiquitin-proteasome system and autophagy, Cells 8 (1) (2019 Jan 10) pii: E40.
[67] M. Høyer-Hansen, L. Bastholm, I.S. Mathiasen, F. Elling, M. Jäättelä, Vitamin D analog EB1089 triggers dramatic lysosomal changes and Beclin 1-mediated autophagic cell death, Cell Death Differ. 12 (2005) 1297–1309.